Atomic-resolution imaging of the polar $(000\bar{1})$ surface of $LiNbO_3$ in aqueous solution by frequency modulation atomic force microscopy

S. Rode,[1] R. Hölscher,[2] S. Sanna,[2] S. Klassen,[1] K. Kobayashi,[3] H. Yamada,[3] W. G. Schmidt,[2] and A. Kühnle[1,*]

[1]*Institut für Physikalische Chemie, Fachbereich Chemie, Johannes Gutenberg-Universität Mainz, Jakob-Welder-Weg 11, 55099 Mainz, Germany*

[2]*Lehrstuhl für Theoretische Physik, Universität Paderborn, 33095 Paderborn, Germany*

[3]*Department of Electronic Science and Engineering, Kyoto University, Katsura, Nishikyo, Kyoto 615-8510, Japan*

(Received 31 March 2012; revised manuscript received 12 June 2012; published 29 August 2012)

Atomic resolution images of the polar $(000\bar{1})$ surface of lithium niobate ($LiNbO_3$) are achieved by frequency modulation atomic force microscopy operated at the solid-water interface. The measured data reveal a hexagonal surface unit cell. Its lattice constant corresponds to the bulk-truncated structure, suggesting that the high-temperature annealed surface does not reconstruct. Compared to the $(000\bar{1})$ surface, high-resolution imaging on the oppositely charged (0001) surface is considerably more difficult to achieve. This finding is rationalized by density functional calculations that indicate a higher corrugation and softer bonds on the $(000\bar{1})$ surface compared to the (0001) surface.

DOI: 10.1103/PhysRevB.86.075468 PACS number(s): 68.08.−p, 68.35.B−, 68.37.Ps, 68.43.−h

I. INTRODUCTION

Lithium niobate [$LiNbO_3$ (LN)] is one of the most versatile materials for optical and acoustic applications due to its unusual piezoelectric, pyroelectric, and photorefractive properties.[1] Below the Curie temperature of 1486 K,[2] LN becomes ferroelectric with a spontaneous polarization along the [0001] direction or c axis; see Fig. 1. Consequently, the $(000\bar{1})$ and the (0001) surfaces of LN are polar and referred to as negative and positive Z cut, respectively. Various stabilization mechanisms are discussed:[3–6] The surfaces may relax, reconstruct, and/or change stoichiometry to generate compensating surface charges. Under ambient conditions or in liquid environment, the adsorption of charged species may additionally screen the surface charge. Due to the ferroelectric nature of LN, the polarity can be inverted by an external electric field. The possibility of switching the spontaneous polarization may lead to very interesting applications, e.g., chemical sensing based on adsorption-induced switching of ferroelectric thin films.[7] Moreover, the LN Z cut has been discussed as a suitable substrate for the epitaxial growth of GaN.[8] In contrast to traditional applications of LN, which mainly rely on its bulk properties, these applications require detailed knowledge about the surface structure and properties. However, only little is known about the surface atomic structure. This is mainly due to the properties of LN itself: An insulating, polar surface of a piezoelectric material poses a number of challenges to surface scientists. Averaging techniques such as low-energy electron diffraction, reflection high-energy electron diffraction, photoelectron spectroscopy, and ion scattering spectroscopy have been applied,[9] but real-space observations have been limited to low-resolution tapping mode atomic force microscopy so far.[10,11] Frequency modulation (FM) atomic force microscopy (AFM) constitutes the method of choice for atomic-resolution imaging of an insulating surface. However, high-resolution FM AFM typically requires operation in an ultrahigh vacuum environment, where unscreened surface charges on polar LN surfaces prohibit high-resolution measurements. In an ambient or liquid environment, in contrast, airborne or waterborne adsorbates can shield the surface charges. Only recently has the FM AFM technique been optimized such that it can now be applied to solid-liquid interfaces,[12,13] demonstrating atomic-resolution capability in aqueous solution.[14,15]

Here we present FM AFM images of the LN$(000\bar{1})$ surface taken in water. The atomic-resolution AFM data reveal a hexagonal surface unit cell, with $p6m$ symmetry for the topmost atomic positions. The experimentally determined lattice constant corresponds to the bulk-truncated structure. Compared to the $(000\bar{1})$ surface, it is found that obtaining high-resolution images is considerably more difficult on the (0001) surface. Density-functional theory (DFT) calculations of the water-LN interface, in contrast, yield water positions that do not depend on the polarity of the surface. The DFT data relate the difference in imaging contrast on the two surfaces to a higher microscopic surface roughness and softer bonds on LN$(000\bar{1})$ compared to LN(0001).

II. EXPERIMENTAL PART

In this study commercially available Z-cut wafers (99-00042-01, Crystal Technology, Inc., USA) are used. Before inserting into the AFM, the samples were cleaned in ethanol and acetone in an ultrasonic bath for 20 min. After cleaning, the samples were annealed at 1273 K for 5 h in a muffle furnace from Nabertherm GmbH (Lilienthal, Germany). Atomic-resolution FM AFM images were obtained in water using an instrument that has been optimized for operation in liquids, having a deflection spectral noise density of below 10 fm/$\sqrt{\text{Hz}}$.[13] All images shown here were taken in an open liquid cell with a volume of approximately 100 μL of Milli-Q water placed above the freshly cleaned surface. The experiments were repeated 19 times for the $(000\bar{1})$ surface and 22 times for the (0001) surface. Care was taken not to contaminate the surface by using ultrasound-cleaned equipment and high-purity water. As force sensors, we used gold-coated, p-doped silicon cantilevers (PPP-NCHAuD from Nanosensors, Neuchâtel, Switzerland) with an eigenfrequency of about 160 kHz, a spring constant of about 40 N/m, and a Q value of around 8 in Milli-Q water (Millipore GmbH,

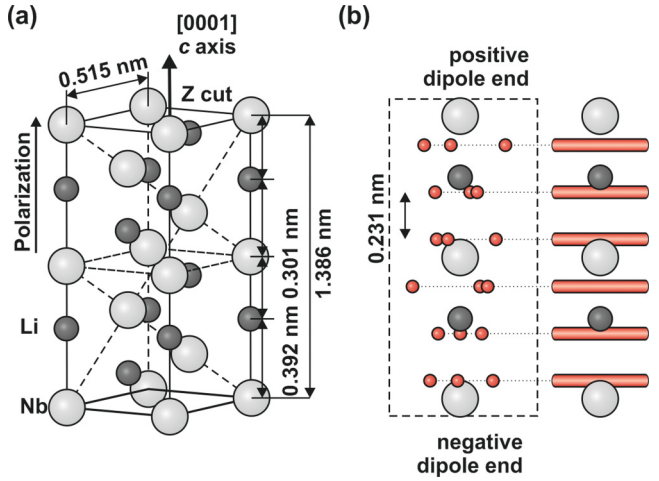

FIG. 1. (Color online) (a) Hexagonal representation of the $LiNbO_3$ unit cell indicating relevant interatomic distances of niobium (white) and lithium (gray) ions of stoichiometric LN. The oxygen atoms are omitted in this model. (b) Positions of the niobium and lithium ions along the [0001] direction relative to the oxygen (small red) ions. (Different sizes are chosen for visualization purpose only.)

Schwalbach, Germany). The cantilever oscillation amplitude was kept constant at a level of around $A = 0.5$–1.7 nm.

An atomically resolved FM AFM image of the $(000\bar{1})$ surface is shown in Fig. 2(a) and the corresponding fast Fourier transformation (FFT) image is given in Fig. 2(b). In order to determine the unit cell structure and dimensions with high accuracy, care was taken to correct the images for drift, as outlined in the following: The drift correction was performed by averaging the FFT of several subsequent images, taken in a series of upward and downward scans. Moreover, for each image set, a forward and a backward scan is collected, thereby canceling out the influence of drift by averaging both upward and downward and forward and backward images. The back transformation of this average FFT representation reveals the drift-corrected real-space dimensions as given in Fig. 2(c). The unit cell is hexagonal with a lattice constant of 0.517 ± 0.02 nm. This value corresponds to the repeat distance in bulk-truncated LN$(000\bar{1})$ and agrees with the surface model obtained from recent DFT calculations;[16,17] see Fig. 2(d).

The (0001) surface was prepared in exactly the same manner as LN$(000\bar{1})$. However, achieving atomic resolution is considerably more difficult than for LN$(000\bar{1})$. A representative image is shown in Fig. 3(a), which is not comparable in quality with the image presented of the LN$(000\bar{1})$ surface. Thus, while atomically resolved images were obtained on the $(000\bar{1})$ surface, the same image quality was not achieved on the (0001) surface. The (0001) surface structure as predicted by DFT (Refs. 16 and 17) is shown in Fig. 3(b).

III. THEORETICAL PART

In order to get insight into the water-LN interaction, total-energy calculations using the VASP implementation of DFT (Ref. 18) are performed. The calculations are on the same footing as previous DFT studies on LN bulk and surface properties.[17,19] We start from the atomic models proposed for the clean LN surfaces in Refs. 17 and 16 that agree with

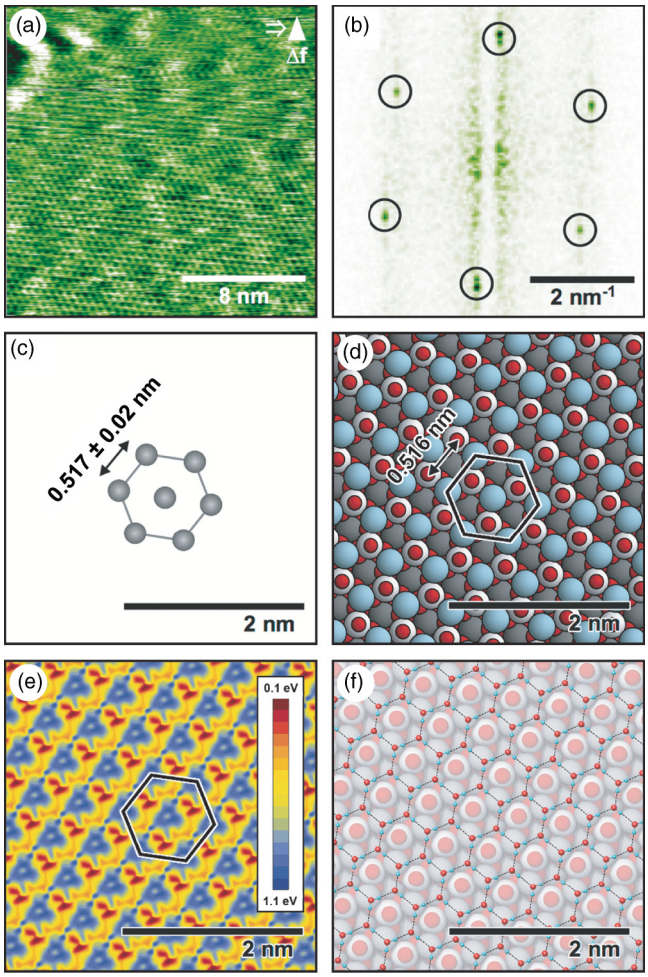

FIG. 2. (Color online) (a) Atomically resolved FM AFM image of the LN$(000\bar{1})$ surface after annealing at 1273 K for 5 h, revealing a hexagonal surface structure. The constant-height image was taken under liquid conditions with a resonance frequency shift of $\Delta f = 1002$ Hz and an oscillation amplitude of $A = 0.62$ nm. (b) Fast Fourier transformations of the image shown in (a). (c) Back transformation of an averaged FFT image, resulting in a drift-corrected unit cell with lattice constant of 0.517 ± 0.02 nm. (d) Top view of the clean $(000\bar{1})$ surface as calculated within DFT (Refs. 16 and 17). Light and dark gray circles indicate up and down Li atoms, while white and small red circles represent Nb and O, respectively. (e) Calculated potential energy surface for the adsorption of single water monomers on the $(000\bar{1})$ surface. (f) Honeycomb structure predicted computationally for the water positions at the liquid-LN$(000\bar{1})$ interface.

the experimental data available so far.[9,20,21] Accordingly, the $(000\bar{1})$ [(0001)] surface is Li-O (Nb-O_3-Li_2) terminated, as shown in Fig. 2(d) [Fig. 3(b)]. The water-LN interfaces are modeled within a 2×2 lateral periodicity using slabs that contain 18 LN substrate atomic layers and are decoupled by about 16 Å in a vacuum.

The potential energy surfaces (PESs) experienced by single water monomers adsorbing on LN $(000\bar{1})$ and (0001) are shown in Figs. 2(e) and 3(c), respectively. In both cases, the calculations predict single water monomers to adsorb close to surface lithium, forming O-Li and H-O bonds between adsorbate and substrate. This leads to relatively large

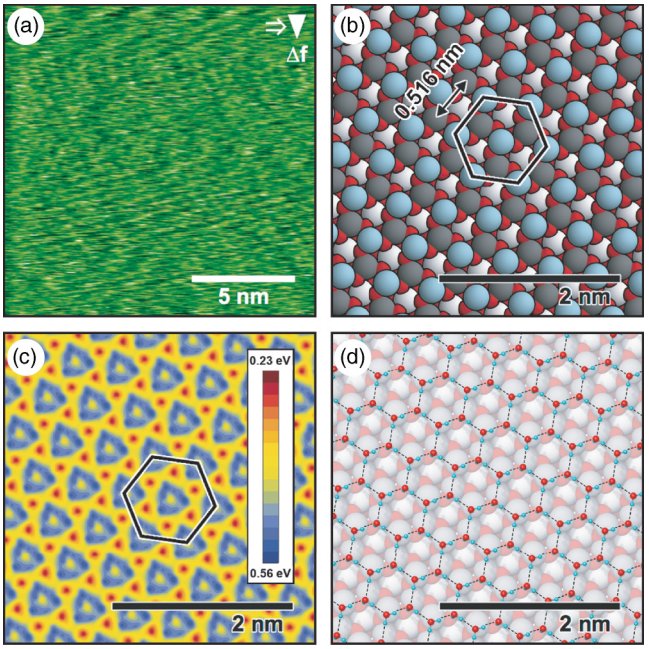

FIG. 3. (Color online) (a) The FM AFM image of the (0001) surface taken in constant-height mode with a resonance frequency shift of $\Delta f = 519$ Hz and an oscillation amplitude of $A = 1.7$ nm. (b) Top view of the clean (0001) surface as calculated within DFT (Refs. 16 and 17). Light and dark gray circles indicate up and down Li atoms, while white and small red circles represent Nb and O, respectively. (c) Calculated potential energy surface for the adsorption of single water monomers on the (0001) surface. (d) Honeycomb structure predicted computationally for the water positions at the liquid-LN(0001) interface.

adsorption energies of 1.1 and 0.6 eV for LN $(000\bar{1})$ and (0001), respectively.

A large number of starting geometries for various water coverages θ ranging from single monomers to thin water films that contain several monolayers (MLs) were probed. Molecular adsorption configurations as well as (partially) dissociated adsorption structures were investigated. In agreement with recent experiments,[22] (i) water adsorption is found to occur nondissociatively and (ii) the relative adsorption energy per water molecule decreases with increasing water coverages.

The grand-canonical potential (see, e.g., Ref. 17) in dependence on the water chemical potential was calculated to determine the stable interface structures. Single molecules, honeycomb films, and multilayer structures are found to be stable on LN$(000\bar{1})$ with increasing water availability. In the case of the LN(0001) surface, the calculations predict the interface to change from an atomically clean surface in a dry environment over regular honeycomb structures to water bilayers and multilayer structures with increasing humidity. Figures 2(f) and 3(d) shows the water monomer positions at the respective interface for $\theta \geqslant 1$ ML. While the PES for single water molecules shown in Figs. 2(e) and 3(c) reflects the symmetry of the clean LN surface, the monomer positions for higher water coverages correspond to the molecular positions at the ice Ih basal plane.[23] Neglecting the protons, the molecular positions have $p3m1$ symmetry for either LN surface.

Interestingly, the DFT data suggest interfacial water positions that are essentially the same for both surface polarizations. However, the adsorption energies differ, which might contribute to the different imaging contrast. A detailed analysis of this effect is, however, beyond the scope of this work. Two other effects were unraveled by the DFT calculations that provide a more straightforward rationale for the different imaging quality. Clearly, the two surfaces have different stoichiometries,[16,17] which lead to different corrugations. In fact, the surface atomic positions on LN$(000\bar{1})$ calculated from DFT give rise to a microscopic surface roughness parameter R_{rms} that is larger (by more than a third) than the corresponding value for LN(0001), 2.5 vs 1.8 Å. This is also reflected in the charge-density corrugations of the two surfaces in the absence [Fig. 4(a)] and presence of water [Figs. 4(b) and 4(c)]. As shown in Fig. 4(b), the presence of water accentuates the surface relaxation but does not qualitatively modify the surface morphology. This is very likely to contribute to the better AFM resolution for LN$(000\bar{1})$. Interestingly, when considering the electronic charge density due to the water molecules, the charge-density plots are changed significantly [Fig. 4(c)]. Indeed, in this case the different surface corrugation of the oppositely polarized surfaces is smoothed out by the presence of the water layer and the two surface charges look very

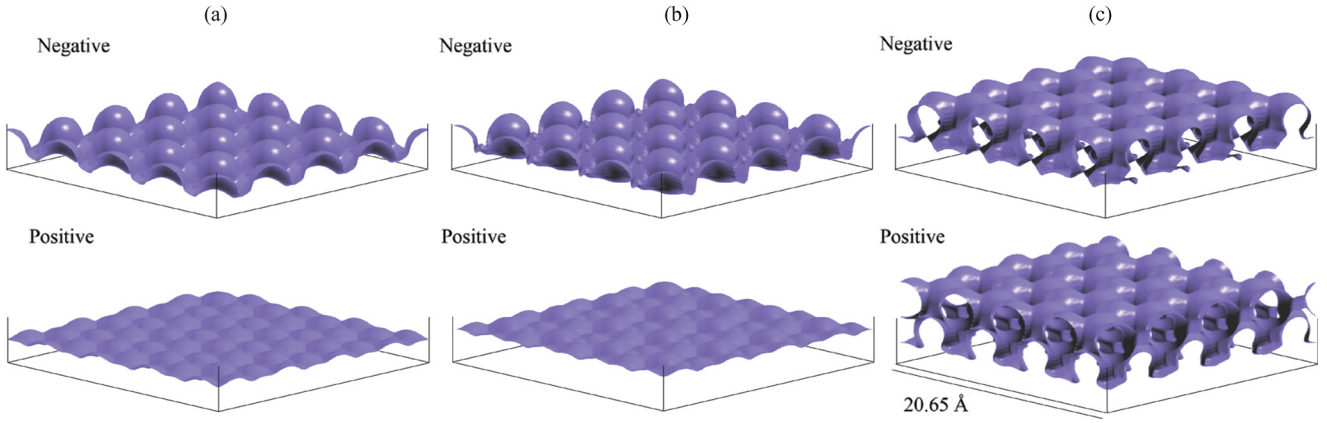

FIG. 4. (Color online) Charge-density isosurface (0.01 $e/\text{Å}^3$) calculated (a) for the clean LN(0001) surface, (b) for the LN(0001) surface in the presence of water, and (c) including water molecules.

similar. This suggests that the surface and not the water layer is imaged by FM AFM, when operated as described above. In addition, the surface bonds are softer on LN(000$\bar{1}$) compared to the (0001) surface, as can be seen in the surface phonon frequencies; see Ref. 24. The vertical surface Li mode on LN(0001), for example, is blue shifted by 61 cm^{-1} with respect to its counterpart on the (000$\bar{1}$) surface. The softer bonds on LN(000$\bar{1}$) are also obvious from the structural relaxation of the surface atoms upon water adsorption, which modifies the surface relaxation and rumpling. On LN(000$\bar{1}$) even the order of the outermost atomic layers changes. While oxygen atoms form the uppermost layer in a vacuum, water film formation drags the Li atoms [light gray in Fig. 3(b)] outward by nearly 1 Å, so that they lie 0.06 Å above the oxygen atoms at the water-LN interface. In contrast, the vertical distance between the uppermost and subsequent layer Li atoms at LN(0001) [shown by light and dark gray in Fig. 3(b)] increases by only 0.25 Å. The considerably softer bonds at the (000$\bar{1}$) surface compared to the (0001) surface are expected to also contribute to higher AFM resolution, as tip-induced surface relaxations are likely to increase the measured corrugation.

IV. CONCLUSION

In conclusion, we have presented high-resolution images of the technologically relevant LN(000$\bar{1}$) surface taken under liquid conditions. A hexagonal unit cell is obtained with a lattice constant that corresponds to the bulk-truncated structure. For the (0001) surface, in contrast, a similar imaging quality was not achieved. To elucidate the origin of these differences in imaging quality, DFT calculations were performed, including an adsorbed water layer. The calculated water positions are essentially the same for both surfaces, yielding no direct evidence for the experimentally observed difference in imaging conditions. This difference is rather related to different stoichiometries, different corrugations, and different bond strengths at the bare substrate surface. Our results (i) indicate that the high-temperature annealed polar (000$\bar{1}$) surface of lithium niobate does not reconstruct and (ii) provide a rationale for the experimentally observed difference in imaging the two polar *Z*-cut surfaces.

ACKNOWLEDGMENTS

We thank the Deutsche Forschungsgemeinschaft (S.S. and W.G.S.) and BASF SE (A.K.) for financial support. The calculations were performed using grants of computer time from the Paderborn Center for Parallel Computing and the HLRS Stuttgart.

*kuehnle@uni-mainz.de

[1] R. S. Weis and T. K. Gaylord, Appl. Phys. A **37**, 191 (1985).
[2] K. K. Wong, *Properties of Lithium Niobate* (The Institution of Electrical Engineers, London, 2002).
[3] C. Noguera, J. Phys.: Condens. Matter **12**, R367 (2000).
[4] T. Jungk, Á. Hoffmann, and E. Soergel, Appl. Phys. Lett. **89**, 042901 (2006).
[5] F. Johann and E. Soergel, Appl. Phys. Lett. **95**, 232906 (2009).
[6] S. V. Kalinin and D. A. Bonnell, Phys. Rev. B **63**, 125411 (2001).
[7] Y. Yun and E. I. Altman, J. Am. Chem. Soc. **129**, 15684 (2007).
[8] G. Namkoong, K. K. Lee, S. M. Madison, W. Henderson, S. E. Ralph, and W. A. Doolittle, Appl. Phys. Lett. **87**, 171107 (2005).
[9] Y. Yun, M. Li, D. Liao, L. Kampschulte, and E. I. Altman, Surf. Sci. **601**, 4636 (2007).
[10] A. Saito, H. Matsumoto, S. Ohnisi, M. Akai-Kasaya, Y. Kuwahara, and M. Aono, Jpn. J. Appl. Phys. **43**, 2057 (2004).
[11] Y. Yun, N. Pilet, U. D. Schwarz, and E. I. Altman, Surf. Sci. **603**, 3145 (2009).
[12] T. Fukuma, M. Kimura, K. Kobayashi, K. Matsushige, and H. Yamada, Rev. Sci. Instrum. **76**, 053704 (2005).
[13] S. Rode, R. Stark, J. Lübbe, L. Tröger, J. Schütte, K. Umeda, K. Kobayashi, H. Yamada, and A. Kühnle, Rev. Sci. Instrum. **82**, 073703 (2011).
[14] T. Fukuma, K. Kobayashi, K. Matsushige, and H. Yamada, Appl. Phys. Lett. **87**, 034101 (2005).
[15] S. Rode, N. Oyabu, K. Kobayashi, H. Yamada, and A. Kühnle, Langmuir **25**, 2850 (2009).
[16] S. V. Levchenko and A. M. Rappe, Phys. Rev. Lett. **100**, 256101 (2008).
[17] S. Sanna and W. G. Schmidt, Phys. Rev. B **81**, 214116 (2010).
[18] G. Kresse and J. Furthmüller, Phys. Rev. B **54**, 11169 (1996).
[19] W. G. Schmidt, M. Albrecht, S. Wippermann, S. Blankenburg, E. Rauls, F. Fuchs, C. Rödl, J. Furthmüller, and A. Hermann, Phys. Rev. B **77**, 035106 (2008).
[20] A. Y. Lushkin, V. B. Nazarenko, K. N. Pilipchak, V. F. Shnyukov, and A. G. Naumovets, J. Phys. D: Appl. Phys. **32**, 9 (1999).
[21] H. Kawanowa, R. Souda, H. Ozawa, Y. Gotoh, K. Terabe, S. Takekawa, and K. Kitamura, Surf. Sci. **538**, L500 (2003).
[22] J. Garra, J. M. Vohs, and D. A. Bonnell, Surf. Sci. **603**, 1106 (2009).
[23] C. Thierfelder, A. Hermann, P. Schwerdtfeger, and W. G. Schmidt, Phys. Rev. B **74**, 045422 (2006).
[24] S. Sanna, G. Berth, W. Hahn, A. Widhalm, A. Zrenner, and W. G. Schmidt, IEEE Trans. Ultrason. Ferr. **58**, 1751 (2011).